

# Tracing high density gas in M 82 and NGC 4038.

E. Bayet<sup>1</sup>, C. Lintott<sup>3</sup>, S. Viti<sup>1</sup>, J. Martín-Pintado<sup>2</sup>, , S. Martín<sup>4</sup>, D.A. Williams<sup>1</sup> and J.M.C. Rawlings<sup>1</sup>

eb@star.ucl.ac.uk

## ABSTRACT

We present the first detection of CS in the Antennae galaxies towards the NGC 4038 nucleus, as well as the first detections of two high-J (5-4 and 7-6) CS lines in the center of M 82. The CS(7-6) line in M 82 shows a profile that is surprisingly different to those of other low-J CS transitions we observed. This implies the presence of a separate, denser and warmer molecular gas component. The derived physical properties and the likely location of the CS(7-6) emission suggests an association with the supershell in the centre of M 82.

*Subject headings:* astrochemistry — ISM: molecules — submillimeter — galaxies: individual (Antennae, M 82) — stars: formation

## 1. Introduction

The molecule CS is a good tracer of dense gas ( $n(\text{H}_2) \geq 10^5\text{-}10^7 \text{ cm}^{-3}$ ) in massive star-forming regions in our own Galaxy (Plume et al. 1992, 1997; André et al. 2007) and in nearby galaxies such as the Magellanic Clouds (Nikolić et al. 2007), M 51 and Maffei 2 (Paglione et al. 1995), NGC 253 (Mauersberger & Henkel 1989; Mauersberger et al. 1989; Martín et al. 2005), IC 342 and M 82 (Henkel & Bally 1985; Mauersberger & Henkel 1989; Mauersberger et al. 1989). Multi-line studies of CS are crucial for the determination of the average gas densities in galaxies since CS transitions have excitation thresholds ranging from  $10^4\text{-}10^5$

---

<sup>1</sup>Department of Physics and Astronomy, University College London, Gower Street, London WC1E 6BT, UK.

<sup>2</sup>Departamento de Astrofísica Molecular e Infrarroja - Instituto de Estructura de la Materia-CSIC, C Serrano 121, E-28006 Madrid, Spain

<sup>3</sup>Oxford Astrophysics, The Denys Wilkinson Building, Keble Road, Oxford OX1 3RH, United Kingdom

<sup>4</sup>Harvard Smithsonian Center for Astrophysics, 60 Garden Street, Cambridge, MA 02138, USA

$\text{cm}^{-3}$  for the CS(2-1) line (Bronfman et al. 1996) up to  $\sim 2 \times 10^7 \text{ cm}^{-3}$  for the CS(7-6) transition (Plume et al. 1992). In this letter, we report in the center of M 82 the first detections of the CS(5-4) and CS(7-6) transitions and the detection of the CS(5-4) line towards the Antennae galaxies (NGC 4038). We have also re-observed lower-J CS lines in M 82. These two well-known sources were chosen because interferometric submillimeter/millimeter maps previously obtained have shown high concentrations of molecular gas. High resolution  $^{12}\text{CO}(1-0)$  maps indicate that the nearby ( $D = 13.8\text{Mpc}$ , see Saviane et al. 2004) Antennae interacting galaxies are likely sites of rapid high mass star formation (Wilson et al. 2000). M 82 represents an excellent example of a nearby ( $D=3.25 \text{ Mpc}$ , see Dumke et al. 2001) starburst galaxy. Low-J molecular line studies (e.g. Fuente et al. 2006; Seaquist et al. 2006; Martín et al. 2006) have determined its average gas physical parameters. However, the molecular emission from the M 82 nucleus appears to come from multiple gas components. In particular the detection of abundant  $\text{CH}_3\text{OH}$  (Martín et al. 2006) and  $\text{HCN}$  (Brouillet & Schilke 1993) indicate the presence of high density gas in the nucleus. Our detection of the CS(7-6) line not only clearly confirms the presence of very high density gas but its analysis (see Sect. 4) suggests that it is located in the expanding superbubble likely to be associated with supernova remnants (Weiß et al. 1999; Wills et al. 1999; Yao et al. 2006).

## 2. Observations and results

The observations of the CS(5-4) line in the Antennae galaxies (NGC 4038 nucleus) and the CS(7-6) transition in M 82 were performed during the spring 2007 at the James Clerk Maxwell Telescope (JCMT). We used a position switching mode under medium weather conditions ( $\tau_{225} = 0.16$ ). For observing the CS(7-6) transition ( $\nu = 342.883\text{GHz}$ ) towards the center of M 82, we used the heterodyne HARP-B multi-beam receiver and the ACSIS digital autocorrelation spectrometers with a bandwidth of 250MHz. The receiver noise temperature (single sideband mode) for the HARP-B central pixel (corresponding to the center of M 82) was  $\sim 344\text{K}$ . The telescope main beam efficiency and half power beam width (HPBW) under this configuration were 0.63 and  $\sim 14''$ , respectively. The CS(5-4) line ( $\nu = 244.936\text{GHz}$ ) has been observed in NGC 4038 and in M 82 using the receivers RxA3 and A3 of the JCMT, respectively, again with the ACSIS 250MHz bandwidth and DAS backends, respectively. The receiver noise temperature (double-side band mode) was 240-450K. The telescope main beam efficiency and HPBW were 0.69 and  $\sim 20''$ , respectively. For both M 82 and NGC 4038, the pointing and calibration were performed carefully on planets (Mars and Jupiter) and on evolved stars. The pointing error was estimated to be  $\leq 2''$  for NGC 4038 whereas is was larger for M 82 ( $< 8-10''$ ).

In the case of M 82, we have also detected the CS(3-2) ( $\nu = 146.969\text{GHz}$ ), the CS(2-1) ( $\nu = 97.980\text{GHz}$ ) and the CS(4-3) ( $\nu = 195.954\text{GHz}$ ) lines with the IRAM-30m in wobbler switching mode on June 1997 and on May 2008. As backend we used a 512 x 1 MHz or the 1024 x 4 MHz filterband. For the CS(3-2) line, the system noise temperature was 300K and the pointing error 2-4'' whereas the CS(2-1) and CS(4-3) lines show  $T_{sys} = 281\text{ K}$  and 1655 K respectively with moderate pointing errors, due to unstable weather conditions. The main beam efficiency and the HPBW of the telescope were 0.69 and  $\sim 17''$  at 147 GHz, 0.75 and  $\sim 25''$  at 97 GHz and 0.63 and  $\sim 13''$  at 195 GHz.

All the data have been reduced using either the GILDAS or the Specx packages, removing the baseline of individual spectra before averaging them. We fitted Gaussian profiles to the resulting spectra (Figs. 1 and 2). In Table 1. As shown in Fig. 1 and Table 1, the most striking result is the narrow line width (only  $40\text{ kms}^{-1}$ ) of the CS(7-6) line in M 82, as compared with those ( $\geq 200\text{ kms}^{-1}$ ) of the lower-J CS transitions (see Sect. 4). Note that both the CS(4-3) and the CS(5-4) intensities and linewidths are dependent on the baseline we removed and thus suffer from large uncertainties, estimated to be up to 20% in the total integrated intensity. However their velocity positions seem robust even if significantly shifted from the expected systemic  $V_{LSR}$  value of M 82 by a factor of 1.3-1.4. Although this characteristic could be explained by instabilities in the pointing, large pointing differences would produce both a shift in velocity and a narrowing in the linewidth, which are not observed. The uncertainties are therefore attributed to the contamination of the observations by the M 82 South West lobe emission at a velocity of  $\sim 100\text{ kms}^{-1}$  (see the CS(2-1) spectrum in Fig. 1).

### 3. The physical properties of the high density gas in M 82 and in NGC 4038

We derive the following integrated line intensity ratios at the center of M 82 :  $r_{32} = \frac{CS(3-2)}{CS(2-1)} = 0.88$ ,  $r_{52} = \frac{CS(5-4)}{CS(2-1)} = 0.37$ . We did not compute the ratio  $r_{72} = \frac{CS(7-6)}{CS(2-1)}$  because the CS(7-6) linewidth is very different from those found for the other lines and seems to imply a different gas component than the one responsible for the lower-J CS transitions (see Sect. 4). Comparing these ratios with those for NGC 253 (see Martín et al. 2005), we found substantial differences. The  $r_{32}$  and  $r_{52}$  ratios in M 82 are around  $3 \times$  the values given for the NGC 253-180 $\text{kms}^{-1}$  component and about  $1.8 \times$  the values given for the NGC 253-280 $\text{kms}^{-1}$  component. These differences probably arise from different gas excitation conditions in the M 82 and NGC 253 nuclei (as already suggested by Bayet et al. 2004, 2006).

Fig. 3 shows the rotation diagram obtained from our observations of CS in M 82, corrected for beam dilution and assuming optically thin emission. As the line profile of the

CS(7-6) transition differs significantly from those of the other lines, and as it is expected that the gas in the nucleus of M 82 is not in thermal equilibrium, we favour a fit with two components, as indicated by the methanol observations of Martín et al. (2006). However, due to the large uncertainties of the CS(4-3) and the CS(5-4) lines, it is also possible to make an acceptable fit of the data with one component. Although we have made a 2-component fit, it is likely that there is a continuous change of the excitation temperature. The rotational temperatures for the 2-component fit are 4.3 K and 16.3 K, respectively, while for the single component fit it is 12.4 K. The rotational temperatures derived from the rotational diagram impose a lower limit to the kinetic temperature of the gas. Thus, the detection of the CS(7-6) transition may require a kinetic temperature ( $T_K$ ) larger than  $\sim 12$ -15K. To estimate the opacity of the CS lines, observations of isotopes of CS are needed. Unfortunately, no isotope detections have been published so far for this position. The effect of the opacity on the rotation diagram is difficult to predict, but it is likely to result in an increase of the derived rotational temperatures.

To constrain the density and the kinetic temperature traced by the detection of CS(7-6) line in M 82, we explored LVG models (Goldreich & Kwan 1974; de Jong et al. 1975). Input parameters ranged from 30 to 100 K for  $T_K$ , from  $10^5\text{cm}^{-3}$  to  $10^8\text{cm}^{-3}$  for  $n(\text{H}_2)$  and from  $1 \times 10^{11}\text{cm}^{-2}$  to  $1 \times 10^{15}\text{cm}^{-2}$  for the CS column density ( $N(\text{CS})$ ). For each model of the grid, we fixed the velocity at the CS(7-6) linewidth value,  $40\text{kms}^{-1}$ . In these LVG models, the CS collision partner is He and the collisional rates used are those from Lique & Spielfiedel (2007). We obtained a good agreement between the observed and modeled CS(7-6) line intensities for a  $T_K$  range of 65-70 K, a  $n(\text{H}_2)$  of  $1.6 \times 10^6\text{cm}^{-3}$  and a  $N(\text{CS})$  of  $1.6 \times 10^{14}\text{cm}^{-2}$ . The source-averaged total CS column density (from the observations) and ranges from  $1.3 \times 10^{13}\text{cm}^{-2}$ - $6.7 \times 10^{14}\text{cm}^{-2}$ , in agreement with LVG model predictions. Comparing our observations with the radiative transfer model of the CS molecule developed by Benedettini et al. (2006), the CS(7-6) observed integrated line intensity could only be reproduced for  $T_K > 50\text{K}$  and  $n(\text{H}_2) \geq 10^6\text{cm}^{-3}$ . Indeed, the best fit was obtained for  $T_K=70\text{K}$  and  $n(\text{H}_2)=10^6\text{cm}^{-3}$  (chemical age of  $2 \times 10^3\text{yr}$ , see Benedettini et al. 2006). This analysis clearly shows that emission from high-J (at least 7-6) CS transitions reveal the presence of very high density gas in M 82.

For the NGC 4038 nucleus, we were not able to perform a similar study as no other transitions of CS were observed towards this source. However, we make a rough estimate the source-averaged total CS column density from the CS(5-4) line in NGC 4038 to be  $N(\text{CS})=1.8 \times 10^{13}\text{cm}^{-2}$ . In both sources, the CS column densities are consistent with our model predictions of gas undergoing high-mass star formation (Bayet et al. 2008) (see Model 15 listed in Table 9). For a more detailed analysis, in a forthcoming paper, we shall compare CS predicted line profiles from chemical models with the observational line profiles presented in this Letter.

#### 4. Discussion

The angular resolution of the CS(7-6) (beam size of 14'') does not allow us to resolve spatially the emitting region. However we can estimate its location from the radial velocity and the velocity width of this line by using the kinematic information provided by interferometric maps of other molecules. Brouillet & Schilke (1993) presented a 2'' resolution HCN(1-0) map of the south west part of M 82. From the channel map of the HCN(1-0) emission centered around  $213.3 \text{ kms}^{-1} (\pm 40 \text{ kms}^{-1})$ , it appears that the CS(7-6) emission may arise from the HCN(1-0) clump located at  $\alpha_{J2000} = 09^h 55^m 52.2^s$  and  $\delta_{J2000} = 69^\circ 40' 46.1''$ , within our beam. García-Burillo et al. (2001, 2002) presented high resolution interferometric HCO and  $\text{H}^{13}\text{CO}^+(1-0)$  maps of M 82. We re-analyzed the data and found that some of the clumps show narrow ( $\leq 60 \text{ kms}^{-1}$ ) emission, similar to that of our CS(7-6) line, confirming the likely location of the CS(7-6) emission at  $\approx (-5'', -2'')$  from the center. This is the location of the expanding molecular supershell (Weiß et al. 1999; Wills et al. 1999; Yao et al. 2006). The high density ( $\geq 10^6 \text{ cm}^{-3}$ ) and the high temperature ( $\approx 60\text{-}80\text{K}$ ) may arise from the interaction between the expanding supershell and the ambient gas in M 82.

In summary, we have presented the first detection of a high density tracer (CS) in the Antennae galaxies (NGC 4038 nucleus) as well as the first detections of two high-J transitions of CS in the center of M 82. We find that multiple molecular gas components in M 82 are necessary to explain the observed line intensities. In particular, while low-J CS lines seem to arise from relatively low density gas ( $\sim 10^5 \text{ cm}^{-3}$ ), the molecular gas traced by the CS(7-6) line must be dense ( $\sim 10^7 \text{ cm}^{-3}$ ) and warm ( $\sim 70\text{K}$ ) and appears to be associated with the expanding supershell in M 82. The high density and temperature may be due to the interaction between the expanding supershell and the ambient gas. Similar multi-line studies

Table 1: Observational parameters.

Source	Line	$\nu$ (GHz)	Tsys (K)	beam size (")	$\int(T_{mb} dv)$ (Kkms $^{-1}$ )	$V_{LSR}$ (Kkms $^{-1}$ )	$\Delta V_{LSR}$ (Kkms $^{-1}$ )	$T_{peak}$ (mK)	rms (mK)
M 82	CS(2-1)	97.980	281	25	$13.3 \pm 0.3$	$221.9 \pm 2.7$	$225.7 \pm 5.4$	55.5	5.8
	CS(3-2)	146.969	303	17	$11.2 \pm 0.3$	$219.7 \pm 2.8$	$211.3 \pm 6.4$	50.1	4.6
	CS(4-3)	195.954	1655	13	$11.1 \pm 1.3$	$161.0 \pm 9.7$	$165.3 \pm 23.2$	63.4	25.8
	CS(5-4)	244.936	437	20	$4.2 \pm 0.8$	$140.0 \pm 38.0$	$211.2 \pm 44.2$	15.6	10.8
	CS(7-6)	342.883	334	14	$2.2 \pm 0.2$	$213.8 \pm 1.5$	$40.1 \pm 2.8$	52.5	14.1
NGC 4038	CS(5-4)	244.936	246	20	$1.7 \pm 0.1$	$1655.0 \pm 4.4$	$98.7 \pm 8.5$	16.3	6.7

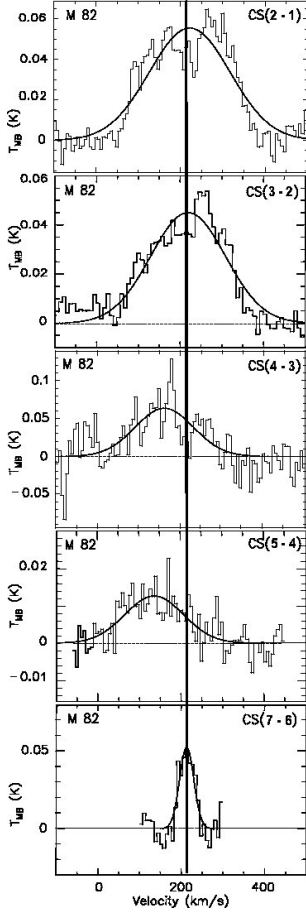


Fig. 1.— Spectra of the CS(2-1), CS(3-2), CS(4-3), CS(5-4) and CS(7-6) lines from top to bottom, respectively, measured towards the center of M 82. The observed position corresponds to the center of M 82 ( $\alpha_{J2000} = 09^h55^m51.9^s$  and  $\delta_{J2000} = +69^\circ40'47''$ ). The CS(2-1) and the CS(4-3) spectra have been smoothed to a common velocity resolution of  $6.1\text{kms}^{-1}$  while the CS(3-2), CS(5-4) and CS(7-6) spectra have a velocity resolution of  $8.2\text{kms}^{-1}$ ,  $\approx 10\text{kms}^{-1}$  and  $6.8\text{kms}^{-1}$ , respectively. The velocity scale (x axis) is expressed in  $\text{kms}^{-1}$  units while the temperature scale (y axis) is expressed in main beam temperature units ( $T_{MB}$ ), converted from the antennae temperature via the main beam efficiencies listed in Sect. 2. The solid black lines superimposed onto each spectrum represents the Gaussian fit while the vertical black line marks the systemic M 82  $V_{LSR}$ .

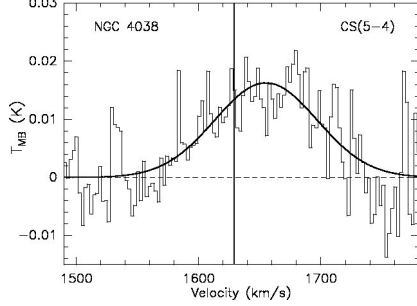


Fig. 2.— Spectrum of the CS(5-4) line towards NGC 4038. The observed position corresponds to the NGC 4038 nucleus ( $\alpha_{J2000} = 12^h01^m52.8^s$  and  $\delta_{J2000} = -18^\circ52'05''$ ). The spectrum has been smoothed to a velocity resolution of  $2.3 \text{ km s}^{-1}$ . The solid black line superimposed on the spectrum represents the Gaussian fit while the vertical black line marks the systemic NGC 4038  $V_{LSR}$ .

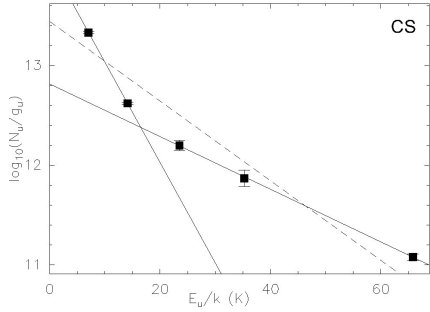


Fig. 3.— Rotation diagram derived from the CS lines towards M 82. The black lines represent the linear regression fits for two gas components while the dashed line corresponds to one single gas component. The black solid squares show the data with error bars. These error bars usually represent the main errors in rotational diagrams which actually correspond to those of the integrated intensities (order of 10-20%). This population diagram has been corrected for beam dilution effects assuming a source size of  $10''$  for the center of M 82. This value is estimated from the interferometric data presented in Brouillet & Schilke (1993) and García-Burillo et al. (2001).

for the Antennae galaxies (NGC 4038/39) are necessary in order to determine the origin of its high density molecular gas component traced by the CS(5-4) line. In both sources, the CS column densities are consistent with model predictions of gas undergoing high-mass star formation (Bayet et al. 2008).

Similar extended multi-transition multi-molecule studies performed on ultra-luminous infra-red galaxies by Greve et al. (2006) and Baan et al. (2008) need to be carried out on nearby sources. In fact, Mühle et al. (2007) presented a detailed study of the para- $\text{H}_2\text{CO}$  in M 82; however this molecule does not trace the dense gas component. Thus, in order to compare the physical and chemical properties of the very dense (extragalactic) gas between ULIRGs and nearby sources, CS observations (from 2-1 to 7-6) of ULIRGs should be performed.

EB acknowledges financial support from the Leverhulme Trust. SV acknowledges individual financial support from STFC AF. This work has been partially supported by the Spanish Ministerio de Educación y Ciencia under projects ESP2004-00665 and ESP2007-65812-C02-01, and “Comunidad de Madrid” Government under PRICIT project S-0505/ESP-0237 (ASTROCAM).

## REFERENCES

- André, P., Belloche, A., Motte, F., & Peretto, N. 2007, *A&A*, 472, 519
- Baan, W. A., Henkel, C., Loenen, A. F., Baudry, A., & Wiklind, T. 2008, *A&A*, 477, 747
- Bayet, E., Gerin, M., Phillips, T. G., & Contursi, A. 2004, *A&A*, 427, 45
- . 2006, *A&A*, 460, 467
- Bayet, E., Viti, S., Williams, D. A., & Rawlings, J. M. C. 2008, *ApJ*, 676, 978
- Benedettini, M., Yates, J. A., Viti, S., & Codella, C. 2006, *MNRAS*, 370, 229
- Bronfman, L., Nyman, L.-A., & May, J. 1996, *A&AS*, 115, 81
- Brouillet, N. & Schilke, P. 1993, *A&A*, 277, 381
- de Jong, T., Dalgarno, A., & Chu, S.-I. 1975, *ApJ*, 199, 69
- Dumke, M., Nieten, C., Thuma, G., Wielebinski, R., & Walsh, W. 2001, *A&A*, 373, 853

- Fuente, A., García-Burillo, S., Gerin, M., Rizzo, J. R., Usero, A., Teyssier, D., Roueff, E., & Le Bourlot, J. 2006, *ApJ*, 641, L105
- García-Burillo, S., Martín-Pintado, J., Fuente, A., & Neri, R. 2001, *ApJ*, 563, L27
- García-Burillo, S., Martín-Pintado, J., Fuente, A., Usero, A., & Neri, R. 2002, *ApJ*, 575, L55
- Goldreich, P. & Kwan, J. 1974, *ApJ*, 189, 441
- Greve, T. R., Papadopoulos, P. P., Gao, Y., & Radford, S. J. E. 2006, *ArXiv Astrophysics e-prints*
- Henkel, C. & Bally, J. 1985, *A&A*, 150, L25
- Lique, F. & Spielfiedel, A. 2007, *A&A*, 462, 1179
- Martín, S., Martín-Pintado, J., Mauersberger, R., Henkel, C., & García-Burillo, S. 2005, *ApJ*, 620, 210
- Martín, S., Mauersberger, R., Martín-Pintado, J., Henkel, C., & García-Burillo, S. 2006, *ApJS*, 164, 450
- Mauersberger, R. & Henkel, C. 1989, *A&A*, 223, 79
- Mauersberger, R., Henkel, C., Wilson, T. L., & Harju, J. 1989, *A&A*, 226, L5
- Mühle, S., Seaquist, E. R., & Henkel, C. 2007, *ApJ*, 671, 1579
- Nikolić, S., Garay, G., Rubio, M., & Johansson, L. E. B. 2007, *A&A*, 471, 561
- Paglione, T. A. D., Jackson, J. M., Ishizuki, S., & Rieu, N. 1995, *AJ*, 109, 1716
- Plume, R., Jaffe, D. T., & Evans, II, N. J. 1992, *ApJS*, 78, 505
- Plume, R., Jaffe, D. T., Evans, II, N. J., Martín-Pintado, J., & Gomez-Gonzalez, J. 1997, *ApJ*, 476, 730
- Saviane, I., Hibbard, J. E., & Rich, R. M. 2004, *AJ*, 127, 660
- Seaquist, E. R., Lee, S. W., & Moriarty-Schieven, G. H. 2006, *ApJ*, 638, 148
- Weiß, A., Walter, F., Neininger, N., & Klein, U. 1999, *A&A*, 345, L23
- Wills, K. A., Redman, M. P., Muxlow, T. W. B., & Pedlar, A. 1999, *MNRAS*, 309, 395

Wilson, C. D., Scoville, N., Madden, S. C., & Charmandaris, V. 2000, *ApJ*, 542, 120

Yao, L., Bell, T. A., Viti, S., Yates, J. A., & Seaquist, E. R. 2006, *ApJ*, 636, 881